Antigelling and Antisickling Bisphenyl Oligopeptides and Peptide Analogues Have Similar Structural Features†

S. K. Burley,*,‡ A. H.-J. Wang,§ J. R. Votano,§ and A. Rich§

Departments of Chemistry and Biology, Massachusetts Institute of Technology, Cambridge, Massachusetts 02139

Received August 26, 1986; Revised Manuscript Received December 31, 1986

ABSTRACT: Single-crystal X-ray diffraction was used to determine the three-dimensional structures of two antigelling oligopeptides, L-lysyl-L-phenylalanyl-L-phenylalanine and L-phenylalanylglycylglycyl-D-phenylalanine, and two antisickling peptide analogues, L-phenylalanine benzyl ester and *N*-phenylacetyl-L-phenylalanine. Although these bisphenyl compounds are chemically quite different from one another, they demonstrate unusual structural similarities: The molecules have compact conformations in which the two phenyl rings are positioned approximately 5 Å apart with interplanar angles approaching 90°, thereby making intramolecular edge-to-face interactions. In addition, the polar atoms, nitrogen and oxygen, are in close proximity without forming intramolecular hydrogen bonds. The relative spatial distribution of polar and nonpolar atoms renders the structures compact and amphipathic. The intramolecular edge-to-face interaction between two aromatic rings, which brings a hydrogen atom with relative positive charge near the π-electron cloud with relative negative charge, is enthalpically favorable and maintains the molecules in a compact and amphipathic conformation. Nonbonded potential energy calculations were used to characterize the energetics of the aromatic–aromatic interaction, and they showed that the observed geometry is stabilized enthalpically by a favorable interaction on the order of −1 to −2 kcal/mol. Structural differences between the two antisickling and the two antigelling agents suggest that molecular volume limits red cell membrane passage. These data provide a molecular structural framework from which to design and synthesize amphipathic bisphenyl compounds that both bind to deoxy sickle cell hemoglobin and cross the erythrocyte membrane.

Sickle cell hemoglobin (HbS)[1] arises in individuals carrying a characteristic mutation in the β-globin gene (β6E → V). On deoxygenation HbS molecules, which differ from deoxyhemoglobin A (HbA) by two additional hydrophobic surface patches, aggregate into double filaments that in turn aggregate in groups of eight to form long fibers about 200 Å in thickness (Bunn & Forget, 1986). These fibers distort the erythrocyte and rigidify the normally flexible cell membrane, thereby altering the cell's hydrodynamic properties and reducing its circulatory half-life.

Unlike most problems of drug design, which seek compounds bound by poorly characterized membrane proteins, the target receptor in sickle cell disease is deoxy-HbS, a globular protein of known structure (Padlan & Love, 1985a,b). Various compounds inhibit deoxy-HbS polymerization by either covalent or noncovalent interactions with the mutant hemoglobin tetramer [for a recent review see Noguchi and Schechter (1985)]. The noncovalently acting compounds include alkylureas (Elbaum et al., 1974) and aromatic compounds, i.e., the amino acids phenylalanine, tyrosine, and tryptophan (Noguchi & Schechter, 1978), phenyl derivatives (Behe & Englander, 1979; Ross & Subramanian, 1977), benzyl esters of aromatic amino acids (Gorecki et al., 1980a), phenoxy and benzyloxy acids (Abraham et al., 1984), and phenylalanine-bearing compounds (Franklin et al., 1983; Gorecki et al., 1980b; Noguchi & Schechter, 1978; Votano & Rich, 1985). NMR and protein crystallographic studies of some of these compounds interacting with deoxy-HbS or deoxy-HbA have characterized distinct binding sites on the macromolecule's surface and have provided some insights into the stereochemical rationale for design of therapeutic agents for sickle cell disease (Russu et al., 1985; Perutz et al., 1986; Abraham et al., 1983, 1984). In addition, chemical comparisons of deoxy-HbS gelation inhibitors have been made and chemical structural templates for the design of possible therapeutic agents have been suggested (Gorecki et al., 1980a; Ross & Subramanian, 1977).

The present investigation extends the template approach through single-crystal X-ray structure determination. L-Lysyl-L-phenylalanyl-L-phenylalanine and L-phenylalanylglycylglycyl-D-phenylalanine, which are bisphenyl agents that inhibit deoxy-HbS gelation, and L-phenylalanine benzyl ester and *N*-phenylacetyl-L-phenylalanine, which can cross the red cell membrane and are bisphenyl antisickling agents, were studied at atomic resolution, and a molecular structural framework from which to design and synthesize possible therapeutic agents for the treatment of sickle cell disease with

† This paper was presented in part at the Ninth American Peptide Symposium, 1985, Toronto, Ontario, Canada. S.K.B. was supported as a Natural Sciences and Engineering Research Council of Canada postdoctoral fellow.

* Address correspondence to this author.

‡ Department of Chemistry. Present address: Department of Medicine, Brigham and Women's Hospital, Boston, MA 02115.

§ Department of Biology.

[1] Abbreviations: Hb, hemoglobin; HbS, sickle cell hemoglobin; HbA, human normal adult hemoglobin; E, L-glutamate; V, L-valine; Val, L-valine; Met, L-methionine; Pro, L-proline; Asp, L-aspartate; Leu, L-leucine; Ser, L-serine; Gly, glycine; Phe, L-phenylalanine; Tyr, L-tyrosine; Trp, L-tryptophan; KFF, L-lysyl-L-phenylalanyl-L-phenylalanine; FGGF, L-phenylalanylglycylglycyl-D-phenylalanine; succinyl-FGGF, succinyl-L-phenylalanylglycylglycyl-D-phenylalanine; FOB, L-phenylalanine benzyl ester; PAF, *N*-phenylacetyl-L-phenylalanine; succinyl-WW, succinyl-L-tryptophanyl-L-tryptophan; e, electrons; Å, angström unit; C_S, concentration of deoxy-HbS in the monomeric phase; C_S/C_S^0, ratio of monomeric deoxy-HbS concentration in the presence of an antigelling agent to monomeric deoxy-HbS concentration in the absence of the antigelling agent; NMR, nuclear magnetic resonance.

0006-2960/87/0426-5091$01.50/0

Table I: Summary of the Crystallographic Data[a]

	KFF	FGGF	FOB	PAF
mol formula	$C_{24}H_{34}N_4O_4 \cdot Br_2$	$C_{22}H_{26}N_4O_5 \cdot 3H_2O$	$C_{15}H_{18}NO_2 \cdot Cl$	$C_{17}H_{17}NO_3$
mol wt	602	462	279	283
crystal system	monoclinic	monoclinic	orthorhombic	orthorhombic
space group	$C2$	$P2_1$	$P2_12_12_1$	$P2_12_12_1$
unit cell				
a (Å)	21.309	5.787	5.221	5.423
b (Å)	5.091	11.786	8.674	8.400
c (Å)	26.589	17.610	33.888	32.548
β (deg)	108.78	104.52		
structure determination	heavy atom phasing (two bromides)	direct methods	heavy atom phasing (chloride)	direct methods
R factor (%)	4.3	5.6	5.2	4.8
unique observations	2270	1849	1247	1199
crystals by	evaporation in aqueous solution	vapor diffusion in 2-methyl-2,4-pentanediol	evaporation in aqueous solution	evaporation in aqueous solution

[a] All bond lengths and angles were within the range of accepted values for peptides (Ramachandran et al., 1974).

noncovalently acting bisphenyl compounds is derived.

Materials and Methods

Peptide Synthesis. The antigelling agents L-lysyl-L-phenylalanyl-L-phenylalanine (KFF) and L-phenylalanyl-glycylglycyl-D-phenylalanine (FGGF) were synthesized as described previously (Gorecki et al., 1980a). The antisickling agents L-phenylalanine benzyl ester (FOB) and *N*-phenylacetyl-L-phenylalanine (PAF) were also synthesized as previously described (Gorecki et al., 1980b; Votano et al., 1984).

Single-Crystal X-ray Structure Determination. A summary of crystallization conditions, crystal system, space group, unit cell dimensions, and method of structure determination is given in Table I. Diffraction measurements were made by using an automated four-circle diffractometer with Cu Kα radiation. All structural models were refined by least-squares methods using SHELX76 (Sheldrick, 1978), and the final crystallographic R factors are given in Table I. Position and anisotropic temperature factors were refined for all nonhydrogen atoms. Hydrogen atoms were located by ideal geometry where possible and allowed to "ride" on the adjacent nonhydrogen atom and an isotropic temperature factor refined. Other hydrogen atoms were located by difference Fourier syntheses and their positions and isotropic temperature factors refined. Final difference Fourier syntheses were calculated, and the average maximum final difference peak was 0.34 e/Å^3 in height. Full crystallographic details with atomic coordinates and temperature factors will be published elsewhere (Wang & Burley, 1987a,b; Fujii et al., 1987; Burley & Wang, 1987).

Deoxyhemoglobin S Preparation. HbS was prepared from heterozygous AS blood as previously described (Votano et al., 1977). The sample was dialyzed for 16 h at 4 °C against deoxygenated buffer [120 mM sodium phosphate (pH 7.2) and 150 mM NaCl]. HbS was concentrated to 35 g/dL by Amicon ultrafiltration using an XM-50 membrane and then stored at 77 K. The percentage of met-HbS never exceeded 4% as determined by the method of Hegesh and Gruener (1970).

Solubility Studies. Solubility ratios were measured by using a method previously described (Votano et al., 1984). The total deoxy-HbS concentration used was 28 g/dL. C_S/C_S^0, the ratio of the monomeric deoxy-HbS concentration in the presence of an agent to the monomeric deoxy-HbS concentration in the absence of the agent, was measured at various concentrations of KFF, succinylated FGGF, and PAF. L-Phenylalanine was used as a control agent so that our measurements could be compared to the work of Poillon (1982). The plotted data are the average of two or three separate measurements. FGGF was succinylated to obtain sufficient solubility (<0.2 M) required for deoxy-HbS solubility measurements and is referred to as succinyl-FGGF. FOB was excluded because of the problem of intermolecular aminolysis at the ester linkage at concentrations greater than 6 mM.

Nonbonded Interaction Energy Calculations. Nonbonded interaction energies for each pair of phenyl rings positioned edge-to-face were calculated by using an approach formulated from ab initio quantum mechanical calculations of dibenzene. The pairwise nonbonded potential energy model for benzene of Karlström et al. (1983) given by

$$E = \sum_{jk}(A_{jk}r^{-1} + B_{jk}r^{-4} + C_{jk}r^{-6} + D_{jk}r^{-9} + E_{jk}r^{-12})$$

was chosen on the strength of its careful and specific development for dibenzene, including reproduction of the experimental dipole and quadrupole moments (Steed et al., 1979; Evans & Watts, 1975). The model was constructed by fitting the above analytic potential function to the results of ab initio quantum mechanical calculations of dibenzene in 72 different relative orientations, some random and some highly symmetric. Each interacting atom pair j,k, separated by distance r_{jk}, is described by parameters A_{jk}, B_{jk}, C_{jk}, D_{jk}, and E_{jk}, which depend on atom types j and k. Some of the terms in the power-series expansion have established physical meanings: r^{-1} is the Coulombic term describing the interaction between partial electronic charges; r^{-6} and r^{-12} are the 6/12 potential terms and describe van der Waals interactions. In practice, the calculation compares the difference between the energy of interaction of the pair of phenyl side chains and that of the same phenyl side chains far apart.

Results

Figures 1 and 2 illustrate ball-and-stick and van der Waals stereo drawings of the molecular structures of KFF, FGGF, FOB, and PAF, respectively designated A–D in each figure. In addition, a summary of the pertinent crystallographic data is given in Table I. The predominant stereochemical feature of these antisickling and antigelling compounds is the edge-to-face interaction involving the two phenyl rings. Although the number of connecting atoms ranges from 5 to 12 and the types of atoms connecting each pair of aromatic groups are highly variable, the phenyl rings assume this close spatial relationship. The center-to-center distance for each ring pair varies between 5.06 and 5.19 Å, with a mean value for all four compounds of 5.11 Å (see Table II). Moreover, this edge-to-face interaction is nearly perpendicular with the angle between the two planes defined by the aromatic rings varying from 70.1 to 82.4°, with a mean value of 76.8° for all compounds (see Table II). In PAF, KFF, and FOB the ortho-hydrogen atom of the carboxy-terminal phenyl ring is in van

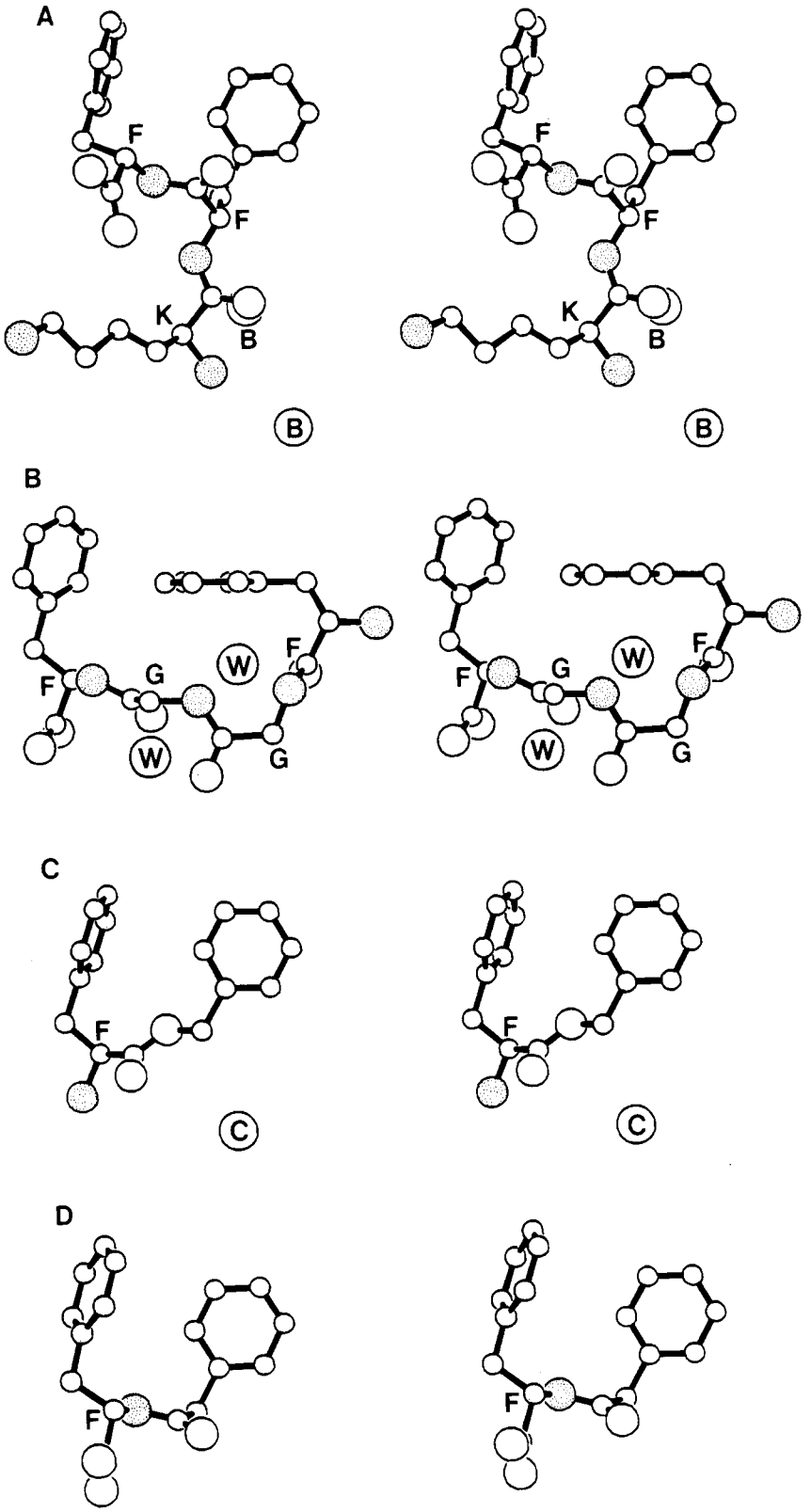

FIGURE 1: Ball-and-stick stereo drawings of the molecular structures of each of the bisphenyl compounds. Small open circles indicate carbon atoms. Large open circles indicate oxygen atoms, and large shaded circles represent nitrogen atoms. Each α-carbon atom is labeled with the appropriate one-letter code signifying amino acid type. Water molecules are indicated with a W and the counterions with a B for bromide and C for chloride. (A) Molecular structure of the antigelling agent L-lysyl-L-phenylalanyl-L-phenylalanine (KFF) with its two bromide counterions. (B) Molecular structure of the antigelling agent L-phenylalanylglycylglycyl-D-phenylalanine (FGGF) with only two of its three bound water molecules included for the sake of clarity. (C) Molecular structure of the antisickling agent L-phenylalanine benzyl ester (FOB) with its chloride counterion. (D) Molecular structure of the antisickling agent *N*-phenylacetyl-L-phenylalanine (PAF).

der Waals contact with the π-electron cloud of the other phenyl group, whereas, in FGGF the para-hydrogen atom is closest to the π-electron cloud of the amino-terminal phenyl group. This edge-to-face interaction, which brings a carbon atom with negative partial charge near a hydrogen atom with positive partial charge, is seen in crystals of benzene and other single-ring aromatic compounds (Cox et al., 1958; Wyckoff, 1969), is enthalpically favorable (calculated nonbonded in-

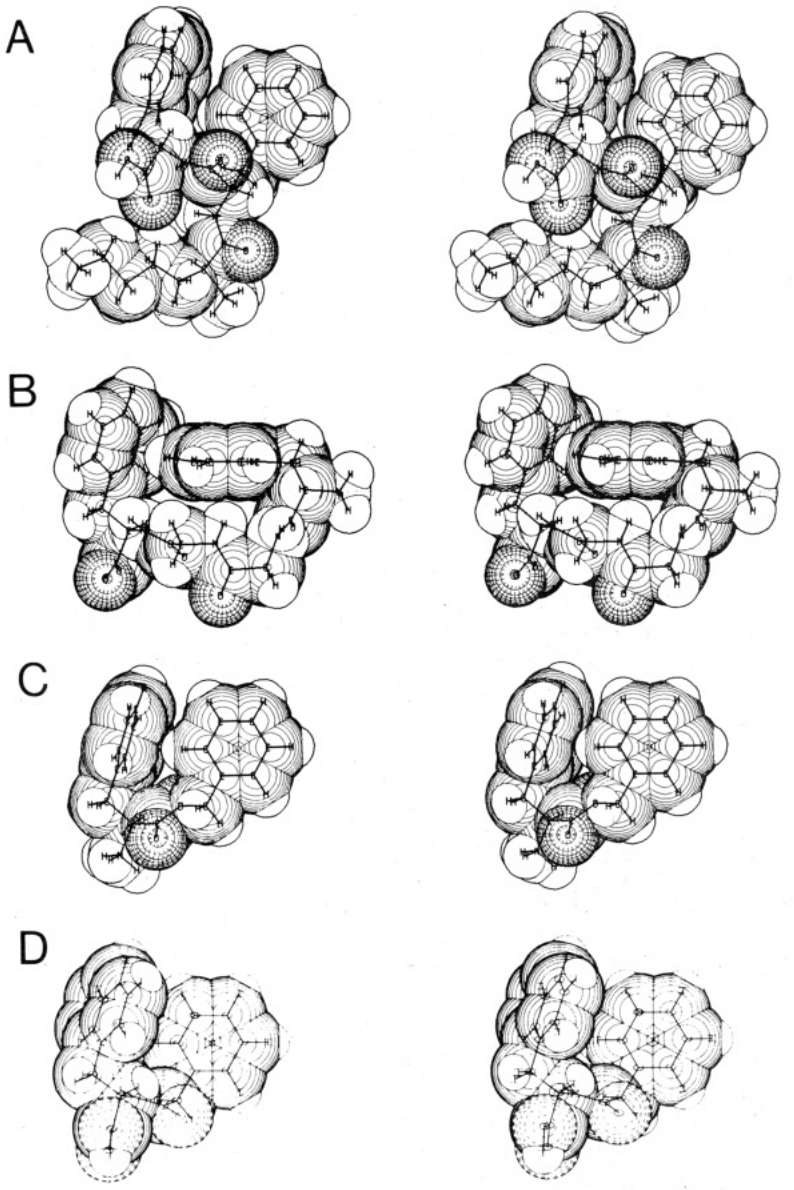

FIGURE 2: van der Waals stereo drawings of the molecular structures of each of the bisphenyl compounds. Each atom type is represented by the following different shading patterns: H atoms, no shading; C atoms, open circles; O atoms, circles with spokes; N atoms, dots. All counterions and water molecules have been omitted for the sake of clarity. (A) Molecular structure of the antigelling agent L-lysyl-L-phenylalanyl-L-phenylalanine (KFF). (B) Molecular structure of the antigelling agent L-phenylalanylglycylglycyl-D-phenylalanine (FGGF). (C) Molecular structure of the antisickling agent L-phenylalanine benzyl ester (FOB). (D) Molecular structure of the antisickling agent *N*-phenylacetyl-L-phenylalanine (PAF).

Table II: Intra- and Intermolecular Edge-to-Face Interactions[a]

compd	donor atom	acceptor ring	*r* (Å)	*D* (deg)	*E* (kcal/mol)
KFF	ortho-H (L-Phe-2)	L-Phe-3	5.19	82.4	−1.86
	meta-H (L-Phe-3)	L-Phe-3′	5.03	76.5	−1.84
	para-H (L-Phe-3′)	L-Phe-2	5.77	47.2	−1.51
FGGF	para-H (L-Phe-1)	D-Phe-4	5.12	75.0	−2.05
	meta-H (D-Phe-4′)	L-Phe-1	4.78	54.3	−2.17
FOB	ortho-H (benzyl)	L-Phe	5.07	79.7	−1.80
	meta-H (L-Phe)	benzyl′	5.00	79.7	−1.86
PAF	ortho-H (phenyl)	L-Phe	5.06	70.1	−1.63
	ortho-H (L-Phe)	phenyl′	4.85	70.1	−2.09

[a] The H atom of closest approach, the σ-donor hydrogen atom, and the π-acceptor aromatic ring are given for each interacting pair with the values of centroid separation (*r*), interplanar angle (*D*), and calculated energy of interaction (*E*). Symmetry-related molecules in the unit cell are indicated by a slanted prime mark.

teraction energies vary between −1.63 and −2.05 kcal/mol, mean = 1.83 kcal/mol, see Table II), and has been described as a weakly polar interaction (Burley & Petsko, 1986a, 1987).

The composite stereo drawings of the four interacting pairs of phenyl rings, illustrated in Figure 3, allow a detailed visual comparison of the intramolecular edge-to-face interactions. Two types of van der Waals contacts between the hydrogen atom of one aromatic ring and the π-electron cloud of the other ring are evident in Figure 3. When the ortho-hydrogen atom is closest to the π-electron cloud, as seen in KFF, FOB, and PAF, the $\delta(+)$ hydrogen atom is positioned near one of the ring-bonding electrons. In FGGF, where the para-hydrogen atom is closest to the π-electron cloud, the $\delta(+)$ hydrogen atom points toward the center of the aromatic ring.

Edge-to-face interactions observed in these four bisaromatic compounds do not depend on the crystallization solvent environment, the presence of bound counterions, water molecules, and bound protons, or the resulting crystal habit. Both aqueous and nonaqueous solvents were used to produce two different crystal systems, orthorhombic and monoclinic, and three different space groups, $P2_12_12_1$, $P2_1$, and $C2$, with markedly different unit cell dimensions. The only exceptions are FOB

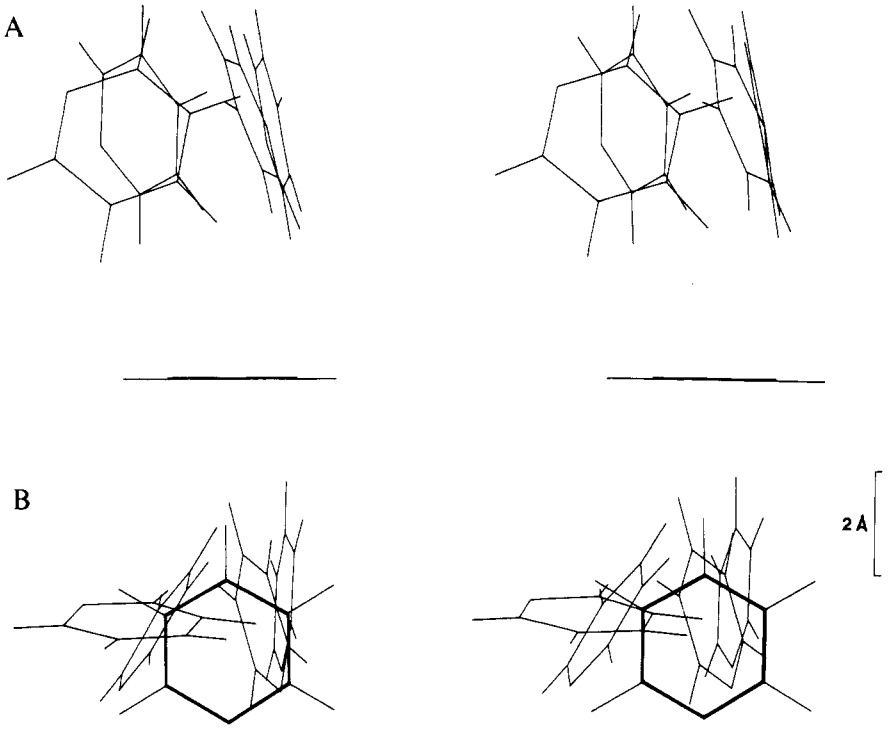

FIGURE 3: Composite stereo drawing of the intramolecular edge-to-face interactions between the four pairs of phenyl rings. Two perpendicular views are illustrated. (A) View along the C_β–C_γ bond of the π-acceptor aromatic ring showing the σ-donor hydrogen atoms sitting above the nearby π-acceptor ring. (B) Perpendicular view looking down the symmetry axis of the aromatic ring, which acts as the π-acceptor.

Table III: Peptide Backbone and Phenylalanine Side-Chain Torsion Angles (Using Standard Definitions)

compd	ϕ (deg)	ψ (deg)	ω (deg)	χ^1 (deg)	$\chi^{2.1}$ (deg)
KFF					
L-Lys-1		145.4	−178.3		
L-Phe-2	−115.4	−53.5	170.4	177.8	81.7
L-Phe-3	−78.8	−9.2		−71.5	−80.7
FGGF					
L-Phe-1		120.6	−171.7	172.4	55.5
Gly-2	−109.6	−12.9	180.0		
Gly-3	−92.1	−149.8	−175.6		
D-Phe-4	73.2	−34.2		62.7	52.9
FOB					
L-Phe		37.5		−171.4	65.9
PAF					
L-Phe	76.8	−19.6	−171.5	−61.2	−72.6

and PAF, which both crystallize in $P2_12_12_1$ with similar unit cell dimensions despite the presence of a chloride counterion in the crystals of FOB and of a proton bound to the carboxylate group of PAF.

Peptide backbone and phenylalanine side-chain torsion angles are given in Table III. Although most of the backbone torsion angles lie within the allowed regions of the Ramachandran diagram (Ramachandran et al., 1963), there are several exceptions: In KFF and FGGF unusual ψ values allow the peptide backbone to bend sharply (L-Phe-3 of KFF ψ = −9.1°, Gly-2 of FGGF ψ = −12.9°, and Gly-3 of FGGF ψ = 149.8°). The ϕ values of all L-amino acid residues in KFF, FGGF, and PAF lie between −76 and −116°, whereas that of D-Phe-4 in FGGF is 73°. L-Phe-2 of KFF, L-Phe-1 of FGGF, and L-Phe of FOB have $\chi^1 \simeq 180°$ and $\chi^{2.1} \simeq 60°$. D-Phe-4 of FGGF has $\chi^1 \simeq 60°$ and $\chi^{2.1} \simeq 60°$, and the remaining L-Phe side chains, L-Phe-3 of KFF and L-Phe of PAF, have $\chi^1 \simeq -60°$ and $\chi^{2.1} \simeq -60°$, which represent L-Phe conformations commonly found in proteins (see Table III).

Figures 1 and 2 demonstrate that these antisickling and antigelling bisphenyl compounds exist as compact and amphipathic molecules. It is remarkable that they adopt this conformation without the aid of stabilizing intramolecular hydrogen bonds. In KFF the lysyl residue is extended, as commonly found in proteins, but is packed against the quasilinear polar peptide backbone without making any hydrogen bonds. In FGGF, FOB, and PAF the peptide backbones are also quasilinear with the polar nitrogen and oxygen atoms projecting away from the two terminal phenyl rings. As stated earlier, the number and type of atoms connecting each pair of phenyl rings are highly variable. The two rings of FGGF are connected by 12 atoms (9 carbons and 3 nitrogens). In KFF 6 atoms connect the two aromatic rings (5 carbons and 1 nitrogen). FOB and PAF both have 5 atoms connecting the two phenyl rings (FOB, 4 carbons and 1 oxygen; PAF, 4 carbons and 1 nitrogen). The segregation of polar atoms and the absence of intramolecular hydrogen bonds render these bisphenyl agents amphipathic. Figure 4, which depicts the crystal-packing behavior of these four compounds, recapitulates the characteristic segregation of polar and nonpolar atoms. The negatively charged counterions, water molecules of crystallization, and nitrogen and oxygen atoms are well separated from the aromatic groups. Most of the possible intermolecular hydrogen bonds are satisified in the polar regions of the crystal, and all possible weakly polar edge-to-face interactions between aromatic groups are satisfied (centroid separations vary between 4.78 and 5.78 Å, mean = 5.11 Å; interplanar angles vary between 47.3° and 79.7°, mean = 65.5°; calculated nonbonded interaction energies vary between −1.51 and −2.17 kcal/mol, mean = −1.89 kcal/mol) (see Table II). The result is a lamellar sandwich of polar and nonpolar atoms not unlike that seen in a lipid bilayer, with the phenyl rings occupying the same positions as the hydrophobic tails of lipid molecules.

A measure of a compound's ability to diminish deoxy-HbS polymerization is given by the solubility ratio of deoxy-HbS in the presence or absence of the antigelling agent (C_S/C_S^0, where C_S is the concentration of deoxy-HbS in monomeric

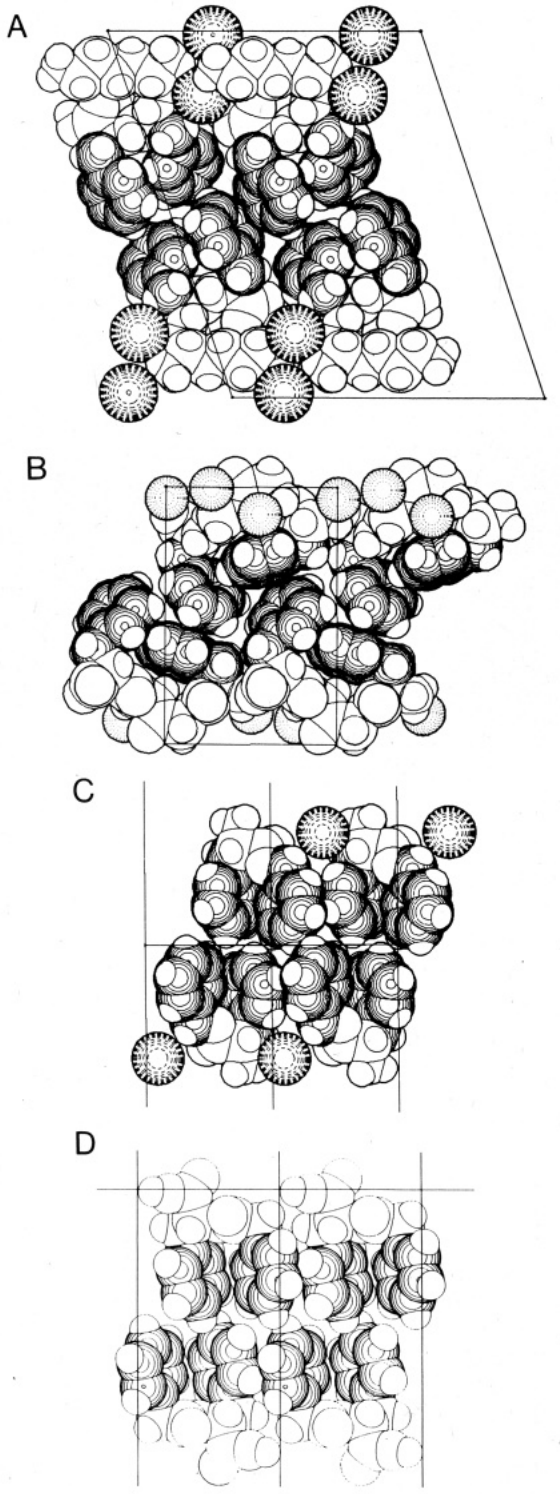

FIGURE 4: van der Waals drawings of the crystal structures of the bisphenyl compounds viewed along the shortest unit cell axis. The C_β and aromatic carbon atoms of the phenylalanine residues are indicated with circle shading. The remaining hydrogen, oxygen, and carbon atoms are not shaded. The counterions that crystallized with KFF and FOB are shaded with spokes only. The three water molecules that crystallized with FGGF are shaded with circles and spokes. (A) Crystal structure of the antigelling agent L-lysyl-L-phenylalanyl-L-phenylalanine (KFF) with two bromide counterions per tripeptide, viewed down the *b* axis. (B) Crystal structure of the antigelling agent L-phenylalanylglycylglycyl-D-phenylalanine (FGGF) with three water molecules per tetrapeptide, viewed down the *a* axis. (C) Crystal structure of the antisickling agent L-phenylalanine benzyl ester (FOB) with one chloride counterion per molecule, viewed down the *a* axis. (D) Crystal structure of the antisickling agent *N*-phenylacetyl-L-phenylalanine (PAF) viewed down the *a* axis. The similarity to the crystal structure of L-phenylalanine benzyl ester, depicted in C, is readily apparent.

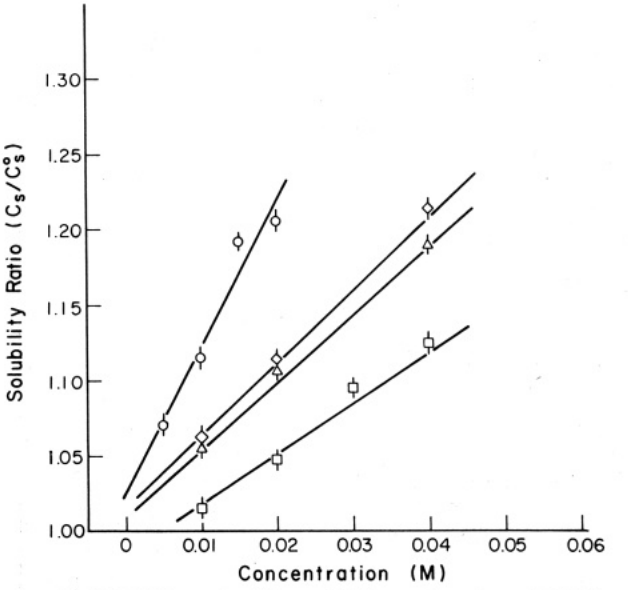

FIGURE 5: Solubility ratio of deoxy-HbS as a function of inhibitor concentration: (○) *N*-phenylacetyl-L-phenylalanine (PAF); (◇) L-lysyl-L-phenylalanyl-L-phenylalanine (KFF); (△) succinyl-L-phenylalanylglycylglycyl-D-phenylalanine (succinyl-FGGF); (□) L-phenylalanine. The linear slopes for PAF, KFF, and succ-FGGF are 3, 1.5, and 1.3, respectively, times that for L-phenylalanine. These data indicate that the bisphenyl compounds are more potent inhibitors of deoxy-HbS gelation than L-phenylalanine.

phase). C_S/C_S^0 values for KFF, PAF, and succinyl-FGGF are given in Figure 5 as a function of the concentration of the bisphenyl compounds. L-Phenylalanine, used as a control, has a slope of 3.1 M^{-1}, which agrees well with the work of Poillon (1982). PAF, KFF, and succ-FGGF have slopes of 9.6, 4.7, and 3.9 M^{-1}, respectively. Although the agents have similar three-dimensional molecular structures, they are not equivalent in their antigelling activity. PAF, which has about twice the molecular volume of the control agent L-phenylalanine and about half the molecular volume of KFF and succinyl-FGGF, is approximately 3 times more effective as a gelation inhibitor than either KFF or succinyl-FGGF. C_S/C_S^0 as a function of FOB concentration is not shown because FOB has poor solution properties and undergoes intermolecular aminolysis at concentrations sufficient to interfere with deoxy-HbS gelation. FOB functions as an antisickling agent by causing the erythrocyte to take up water after the bisphenyl compound has traversed the red cell membrane (Votano et al., 1984).

Discussion

Intramolecular Interactions. A principal objective of this study was to ascertain if there are structural features common to these diverse bisaromatic compounds, given that KFF, succinyl-FGGF, and PAF have antigelling activity and that PAF and FOB display two distinct modes of antisickling activity. To our surprise all four compounds were found to be compact and amphipathic. More important, this unusual conformation is stabilized by a weakly polar, enthalpically favorable edge-to-face interaction between their two aromatic rings. Although, in the case of small peptides, no bisphenyl peptide structures with intramolecular edge-to-face interactions were detected in a survey of the Cambridge Crystallographic Data Base (data not shown), such intramolecular edge-to-face interactions do exist in globular proteins (Burley & Petsko 1985, 1986a; Singh & Thornton, 1985). A NMR spectroscopic study of somatostatin by Hirschmann and co-workers (Arison et al., 1981) revealed that the side chains of L-phenylalanine-6 and L-phenylalanine-11 have this edge-to-face

configuration, and a similar interaction exists between L-tyrosine-2 and L-phenylalanine-3 in the single-crystal structure of pressionic acid (Langs et al., 1986). In the latter compound, the para-hydrogen atom of L-Phe-3 is in van der Waals contact with the π-electron cloud of L-Tyr-2, with a 6-atom spacing between rings. Although the intramolecular edge-to-face interaction between rings may appear unusual at first glance, it is analogous to the well-known crystal structure of benzene (Cox et al., 1958). Such intramolecular interactions are enthalpically favorable provided that there are no electron-withdrawing or -donating substituents attached to the ring, which alter the distribution of positive and negative partial charges, and that the compound's backbone is sufficiently flexible so as to permit close approach of the two rings.

Intermolecular Interactions. The weakly polar behavior of interacting phenyl rings described above suggests that aromatic groups can engage in a variety of enthalpically favorable intermolecular interactions, which result from the characteristic segregation of positive and negative partial charges in the ring system. For example, groups carrying negative charge can interact with the $\delta(+)$ hydrogen atoms of an aromatic ring. Carbonyl oxygen atoms, which have negative partial charge, can make electrostatic interactions with nearby hydrogen atoms of aromatic rings with energies of between -1 and -2 kcal/mol. Such interactions have been identified both in small-molecule crystal structures of phenylalanine (Gould et al., 1985) and in protein structures where they represent a mechanism of protein structure stabilization (Thomas et al., 1982). Their formation does not preclude hydrogen bonding between the carbonyl oxygen and a nearby nitrogen or oxygen atom because there are two lone pairs of electrons on each carbonyl oxygen, one available for hydrogen bonding and the other available for another hydrogen bond or an additional electrostatic interaction. Electronegative sulfur atoms, found in the amino acids methionine and cysteine, are also thought to make enthalpically favorable electrostatic interactions with the $\delta(+)$ hydrogen atoms of aromatic side chains (Reid et al., 1985). In addition, groups carrying positive charge can interact with the $\delta(-)$ π-electron cloud of an aromatic ring. Positively charged or $\delta(+)$ side-chain amino groups, found in the amino acids lysine, arginine, asparagine, glutamine, and histidine, can engage in electrostatic interactions with the $\delta(-)$ π-electron clouds of aromatic side chains as observed in proteins (Burley & Petsko, 1986b). This interaction is analogous to the enthalpically favorable interaction between NH_4^+ and the π-electron cloud of benzene characterized by ab initio quantum mechanical calculations (Deakyne & Moet-Ner (Mautner), 1985). Finally, intermolecular edge-to-face interactions can occur between aromatic groups of different molecules. Such interactions are depicted in Figure 4, which shows KFF, FGGF, FOB, and PAF in their crystal environments. Gould et al. (1985) made a survey of phenyl–phenyl interplanar angles in L-phenylalanine crystal structures and documented a similar pattern of intermolecular edge-to-face interactions. For a detailed review of the subject of weakly polar interactions in proteins, see Burley and Petsko (1987).

Proposed Antigelling Mechanism. We suggest that PAF, KFF, and FGGF inhibit deoxy-HbS gelation by interacting with a nonpolar site or sites on the surface of the deoxy-HbS tetramer. Competitive binding studies of various structurally and chemically related bisaromatic compounds, including succinyl-FGGF, have documented the existence of a pair of strongly preferred binding sites on both the deoxy-HbA and deoxy-HbS tetramers, and the bisaromatics bind to the two hemoglobin tetramer sites with energies of about -3.0 kcal/mol (Votano & Rich, 1985). We believe that the primary impetus for noncovalent binding of the compact, amphipathic bisphenyl compounds of deoxy-HbS is the hydrophobic effect, and interaction with the deoxy-HbS tetramer will almost certainly displace some hydrogen-bonded water molecules from both the ligand and the surface of the protein. Hence, the free energy of ligand binding will be the sum of the entropic contribution and the enthalpic contribution, which is a function of both van der Waals and electrostatic interactions. Such electrostatic interactions can range from hydrogen bonds to weaker interactions between molecular dipole and quadrupole moments.

Although we have not determined the locations of the two major sites at which the bisphenyl agents bind to the deoxy-hemoglobin tetramers, a recent crystallographic study by Perutz et al. (1986) has located two sites on deoxy-HbA where succinyl-L-tryptophanyl-L-tryptophan (succinyl-WW) binds. This bisaromatic compound was synthesized during our earlier studies of antigelling agents (Gorecki et al., 1980a) and, when bound to deoxy-HbA, it has a compact, amphipathic structure that resembles the molecular structures of these four bisphenyl agents. The $\delta(+)$ $\epsilon 3$ and $\zeta 3$ hydrogen atoms of L-Trp-3 are in van der Waals contact with the $\delta(-)$ π-electron cloud of the indole moiety of L-Trp-2, and the backbone polar atoms are spatially segregated from the two aromatic groups. Two succinyl-WW molecules are in contact and bind to a symmetry-related pair of sites in the central cavity of the deoxy-HbA tetramer in the vicinity of residues Val NA1 (1), Leu NA2 (2), Val EF2 (73), Asp EF3 (74), Met EF5 (76), Pro EF6 (77), and Ser H14 (131) of the α-chains. This portion of the deoxy-HbA tetramer is isomorphous to the same region in deoxy-HbS and far from any intermolecular contact site in the deoxy-HbS polymer (Padlan & Love, 1985a,b). Three hydrogen bonds per ligand and numerous weakly polar and van der Waals interactions between succinyl-WW and globin and also between the two succinyl-WW molecules are responsible for ligand binding. Succinyl-WW binding alters the local structure of the binding sites and appears to alter the outer surface of the deoxy-HbA tetramer in a subtle way so as to increase its solubility. We presume that similar changes to the deoxy-HbS tetramer also affect its aggregation equilibrium and thereby inhibit gelation.

While we do not know the structures of the antigelling agents PAF, KFF, and succinyl-FGGF complexed to deoxy-Hb, the structural similarity to each other and to succinyl-WW makes it reasonable for us to suggest that they may be binding at the pair of sites in the central cavity identified by Perutz et al. (1986). Moreover, since the structures are not identical in detail, it is not surprising that there are differences as large as 3-fold in the potency of PAF, KFF, and succinyl-FGGF.

Erythrocyte Membrane Passage. Intracellular uptake of a compound may not only allow targeting of the deoxy-HbS tetramer by the compound but also stimulate red cell swelling due to water gain by the cell in the process of reestablishing the chemical equilibrium across its membrane. Small increases, around 10%, in corpuscular volume can lengthen by several orders of magnitude the delay time of deoxy-HbS aggregation (Votano et al., 1984), even with only small increases in deoxy-HbS solubility due to the action of a chemical agent. The structural data we report here provide insight into the problem of designing bisphenyl compounds capable of passing through the red blood cell membrane. FOB and PAF, which are positively or negatively charged at neutral pH, respectively, readily penetrate the erythrocyte membrane, whereas KFF, which is positively charged at pH 7.0, and

FGGF, which exists as a zwitterion at neutral pH, cannot enter the red blood cell. These findings indicate that neither amphipathic conformation, the result of enthalpically favorable edge-to-face interactions between phenyl rings, nor net molecular charge at physiologic pH limits membrane passage. Instead, it appears that the size and, to a lesser extent, the hydrophobic content of the compound play important roles in determining cellular permeability. FOB and PAF have molecular volumes of about 550 Å^3, which is substantially smaller than the value of 900 Å^3 obtained for KFF and FGGF. FOB and PAF are about 70% carbon atoms by volume, whereas KFF and FGGF are about 62% carbon atoms by volume. Both FOB and PAF, which have comparable molecular volumes, are permeable in spite of the presence of four atoms capable of hydrogen bonding on PAF and only three on FOB, whereas KFF and FGGF, which have approximately twice the molecular volume of PAF and eight and nine atoms capable of hydrogen bonding, respectively, do not cross the erythrocyte membrane.

Molecular Structural Framework. Binding of any compound to the deoxy-Hb tetramer is predicated on several important stereochemical considerations: (i) the hydrophobic character of the compound itself; (ii) the van der Waals space available at the surface of the deoxy-Hb tetramer; and, as stated by Perutz et al. (1986), (iii) the compound's potential for making a large number of the electrostatic interactions with nearby atoms at the protein's surface. The four bisphenyl compounds described above constitute a unique molecular structural framework from which to design potential noncovalently acting therapeutic agents for the treatment of sickle cell disease. Parameters open to optimization include the following:

(i) Compound size and hydrophobicity, which affect both delivery and drug binding at specific sites on the deoxy-Hb tetramer, can be varied by altering the number and types of connecting atoms between the two phenyl rings without significantly perturbing the edge-to-face interaction that maintains the compact, amphipathic nature of these agents.

(ii) The relative insensitivity of the edge-to-face interaction to the precise length and composition of the connecting backbone will also permit independent optimization of the hydrogen bonds involving backbone atoms and the numerous weakly polar interactions involving molecular dipole and quadrupole moments.

Finally, when the geometric and stereochemical features of the bisphenyl compounds binding to deoxy-Hb have been elucidated, it should be possible to determine some of the aspects of deoxy-Hb–ligand binding that affect the potency of deoxy-HbS gelation inhibition. It is clear that we do not understand the fundamental mechanism of gelation inhibition. However, structural analyses may provide clues to help us develop potential therapeutic agents for the treatment of sickle cell disease using noncovalently acting bisaromatic compounds.

ACKNOWLEDGMENTS

We thank Drs. G. A. Petsko and R. F. Tilton, Jr., for their useful discussion and comments on the manuscript. In addition, we thank Drs. J. Singh and J. M. Thornton for early transmission of their study of phenylalanine interactions in proteins.

Registry No. KFF, 63912-10-7; FGGF, 97762-34-0; FOB, 962-39-0; PAF, 738-75-0; HbS, 9035-22-7.

REFERENCES

Abraham, D. J., Mehanna, A. S., & Williams, F. L. (1982) *J. Med. Chem. 25*, 1015–1020.

Abraham, D. J., Perutz, M. F., & Phillips, S. E. V. (1983) *Proc. Natl. Acad. Sci. U.S.A. 80*, 324–328.

Abraham, D. J., Kennedy, P. E., Mehanna, A. S., Patwa, D. C., & Williams, F. L. (1984) *J. Med. Chem. 27*, 967–978.

Arison, B. H., Hirschmann, R., Paleveda, W. J., Brady, S. F., & Veber, D. F. (1981) *Biochem. Biophys. Res. Commun. 100*, 1148–1163.

Behe, M. J., & Englander, S. W. (1979) *Biochemistry 18*, 4196–4201.

Bunn, H. F., & Forget, B. G. (1986) *Hemoglobin: Molecular, Genetic and Clinical Aspects*, W. B. Saunders, Philadelphia, PA.

Burley, S. K., & Petsko, G. A. (1985) *Science (Washington, D.C.) 229*, 23–28.

Burley, S. K., & Petsko, G. A. (1986a) *J. Am. Chem. Soc. 108*, 7995.

Burley, S. K., & Petsko, G. A. (1986b) *FEBS Lett. 203*, 139–143.

Burley, S. K., & Petsko, G. A. (1987) *Adv. Protein Chem.* (in press).

Burley, S. K., & Wang, A. H.-J. (1987) *Acta Crystallogr., Sect. C: Cryst. Struct. Commun. 43*, 797–799.

Cox, E. G., Cruickshank, D. W. J., & Smith, J. A. S. (1958) *Proc. R. Soc. London, Ser. A 247*, 1–16.

Deakyne, C. A., & Moet-Ner (Mautner), M. (1985) *J. Am. Chem. Soc. 107*, 474–479.

Elbaum, D., Nagel, R. L., Bookchin, R. M., & Herskovits, T. T. (1974) *Proc. Natl. Acad. Sci. U.S.A. 71*, 4718–4722.

Evans, D. J., & Watts, R. O. (1975) *Mol. Phys. 29*, 777–782.

Franklin, I. M., Cotter, R. I., Cheetham, R. C., Pardon, J. F., Hale, A. J., & Huehns, E. R. (1983) *Eur. J. Biochem. 136*, 209–214.

Fujii, S., Burley, S. K., & Wang, A. H.-J. (1987) *Acta Crystallogr., Sect. C: Cryst. Struct. Commun. 43*, 1008–1009.

Gorecki, M., Acquaye, C. T. A., Wilchek, M., Votano, J. R., & Rich, A. (1980a) *Proc. Natl. Acad. Sci. U.S.A. 77*, 181–185.

Gorecki, M., Votano, J. R., & Rich, A. (1980b) *Biochemistry 19*, 1564–1568.

Gould, R. O., Gray, A. M., Taylor, P., & Walkinshaw, M. D. (1985) *J. Am. Chem. Soc. 107*, 5921–5927.

Hegesh, E., & Gruener, N. (1970) *Clin. Chim. Acta 36*, 679–686.

Karlström, G., Linse, P., Wallqvist, A., & Jönsson, B. (1983) *J. Am. Chem. Soc. 105*, 3777–3782.

Langs, D. A., Smith, G. D., Stezowski, J. J., & Hughes, R. E. (1986) *Science (Washington, D.C.) 232*, 1240–1242.

Noguchi, C. T., & Schechter, A. N. (1978) *Biochemistry 17*, 5455–5459.

Noguchi, C. T., & Schechter, A. N. (1985) *Annu. Rev. Biophys. Biophys. Chem. 14*, 239–263.

Padlan, E. A., & Love, W. E. (1985a) *J. Biol. Chem. 260*, 8272–8279.

Padlan, E. A., & Love, W. E. (1985b) *J. Biol. Chem. 260*, 8280–8291.

Perutz, M. F., Fermi, G., Abraham, D. J., Poyart, C., & Bursaux, E. (1986) *J. Am. Chem. Soc. 108*, 1064–1078.

Poillon, W. N. (1982) *Biochemistry 21*, 1400–1406.

Ramachandran, G. N., Ramakrishnan, C., & Sasisekharan, V. (1963) *J. Mol. Biol. 7*, 95–99.

Ramachandran, G. N., Kolaskar, D., Ramakrishnan, C., & Sasisekharan, V. (1974) *Biochim. Biophys. Acta 359*, 298–317.

Reid, K. S. C., Lindley, P. F., & Thornton, J. M. (1985) *FEBS Lett. 190*, 209–213.
Ross, P. D., & Subramanian, S. (1977) *Biochem. Biophys. Res. Commun. 77*, 1217–1223.
Russu, I. M., Lin, A. K.-L. C., Yang, C.-P., & Ho, C. (1986) *Biochemistry 25*, 808–815.
Sheldrick, G. M. (1978) in *Computing in Crystallography* (Schenk, H., Olthof-Hazekamp, R., van Koningsveld, H., & Bassi, G. C., Eds.) pp 34–42, Delft Univeristy, Delft, The Netherlands.
Singh, J., & Thornton, J. M. (1985) *FEBS Lett. 191*, 1–6.
Steed, J. M., Dixon, T. A., & Klemperer, W. J. (1979) *J. Chem. Phys. 70*, 4940–4944.
Thomas, K. A., Smith, G. M., Thomas, T. B., & Feldman, R. J. (1982) *Proc. Natl. Acad. Sci. U.S.A. 79*, 4843–4847.
Votano, J. R., & Rich, A. (1985) *Biochemistry 24*, 1966–1970.
Votano, J. R., Gorecki, M., & Rich, A. (1977) *Science (Washington, D.C.) 196*, 1216–1218.
Votano, J. R., Altman, J., Wilchek, M., Gorecki, M., & Rich, A. (1984) *Proc. Natl. Acad. Sci. U.S.A. 81*, 3190–3194.
Wang, A. H.-J., & Burley, S. K. (1987a) *Acta Crystallogr., Sect. C: Cryst. Struct. Commun.* (in press).
Wang, A. H.-J., & Burley, S. K. (1987b) *Acta Crystallogr., Sect. C: Cryst. Struct. Commun. 43*, 1011–1012.
Wyckoff, R. W. G. (1969) *Crystal Structures, The Structure of Benzene Derivatives*, Interscience, New York.

Determination of Lipid Asymmetry in Human Red Cells by Resonance Energy Transfer†

Jerome Connor and Alan J. Schroit*
Department of Cell Biology, The University of Texas M. D. Anderson Hospital and Tumor Institute at Houston, Houston, Texas 77030

Received February 13, 1987; Revised Manuscript Received April 8, 1987

ABSTRACT: This report describes the application of a resonance energy transfer assay to determine the transbilayer distribution of 7-nitro-2,1,3-benzoxadiazol-4-yl (NBD)-labeled lipid analogues. The validity of this technique was established by determining the relationship between the distance of separation of lissamine rhodamine B labeled phosphatidylethanolamine (*N*-Rho-PE) acceptor lipid and NBD-labeled donor lipid and energy transfer efficiency. By determination of the distance between probes at 50% transfer efficiency (R_0), the distance between fluorophores distributed symmetrically (outer leaflet label) and asymmetrically in artificially generated vesicles was determined. Calculation of the average distance between probes revealed a 14-Å difference between NBD-lipid and *N*-Rho-PE localized in the same leaflet and in opposing leaflets, respectively. Application of this technique to the study of the transbilayer distribution of NBD-lipid in human red blood cells (RBC) showed that exogenously supplied NBD-phosphatidylserine (NBD-PS) was selectively transported to the inner leaflet, whereas NBD-phosphatidylcholine remained in the outer leaflet. In contrast, pretreatment of the RBC with diamide (a SH cross-linking reagent) blocked the transport of NBD-PS. The absence or presence of NBD-PS in the outer leaflet was independently verified by employing "back-exchange", trinitrobenzenesulfonic acid derivatization, and decarboxylation with PS decarboxylase experiments. These control experiments yielded results which confirmed the lipid distributions determined by the resonance energy transfer assay.

It has been established that anionic phospholipids such as phosphatidylethanolamine (PE)[1] and phosphatidylserine (PS) are asymmetrically distributed in biological membranes (Rothman & Lenard, 1977; Op den Kamp, 1979). In red blood cells (RBC), the aminophospholipids preferentially reside in the inner leaflet, while the choline phospholipids are predominantly localized in the outer leaflet (Verkleij et al., 1973; Gordesky et al., 1975). Both the biogenesis and the maintenance of this phospholipid asymmetry appear to be important components of homeostasis since the translocation of lipids between leaflets has been implicated in several important biological processes. For example, translocation of PS in activated platelets (Bevers et al., 1983) and sickle RBC (Chiu et al., 1979; Lubin et al., 1981) has been shown to be important in clotting mechanisms (Bevers et al., 1982) and in the pathogenesis of sickle cell anemia (Schwartz et al., 1985; Franck et al., 1985), respectively. In addition, PS has been shown to be an important factor in macrophage recognition of both artificial (Schroit & Fidler, 1982) and biological membranes (Tanaka & Schroit, 1983; Schroit et al., 1985). Since monitoring unlabeled endogenous lipid translocation (inner to outer leaflet) is difficult, alternative methods have recently been introduced that follow the fate of exogenous lipids inserted into

† This work was supported in part by Developmental Fund Grant 175416 from The University of Texas M. D. Anderson Hospital and Tumor Institute at Houston and by National Institutes of Health Grant CA-40149.

[1] Abbreviations: DOPC, dioleoylphosphatidylcholine; HEPES saline, 145 mM NaCl, 5 mM KCl, 20 mM HEPES, and 10 mM glucose; HEPES, *N*-(2-hydroxyethyl)piperazine-*N*′-2-ethanesulfonic acid; LUV, large unilamellar vesicle(s); *N*-Rho-PE, *N*-(lissamine rhodamine B sulfonyl)phosphatidylethanolamine; NBD-PC and -PS, 1-oleoyl-2-[[*N*-(7-nitro-2,1,3-benzoxadiazol-4-yl)amino]caproyl]phosphatidylcholine and -phosphatidylserine, respectively; PSdC, phosphatidylserine decarboxylase; RBC, human red blood cells; SUV, small unilamellar vesicle(s); TLC, thin-layer chromatography; TNBS, trinitrobenzenesulfonic acid; Tnp, trinitrophenyl; ^{125}I-PE, *N*-[3-(3-[^{125}I]iodo-4-hydroxybenzyl)-propionyl]dipalmitoylphosphatidylethanolamine; RET, resonance energy transfer.

0006-2960/87/0426-5099$01.50/0